

# Optimal Control for a COVID-19 and Tuberculosis Co-Infection Model with Asymptomatic COVID-19 Carriers

Sailah Ar Rizka et al.



Volume 13, Issue 1, Pages 84–95, April 2025

Received 28 February 2025, Revised 19 April 2025, Accepted 23 April 2025, Published 25 April 2025

To Cite this Article : S. A. Rizka et al., “Optimal Control for a COVID-19 and Tuberculosis Co-Infection Model with Asymptomatic COVID-19 Carriers”, *Euler J. Ilm. Mat. Sains dan Teknol.*, vol. 13, no. 1, pp. 84–95, 2025, <https://doi.org/10.37905/euler.v13i1.31076>

© 2025 by author(s)

## JOURNAL INFO • EULER : JURNAL ILMIAH MATEMATIKA, SAINS DAN TEKNOLOGI

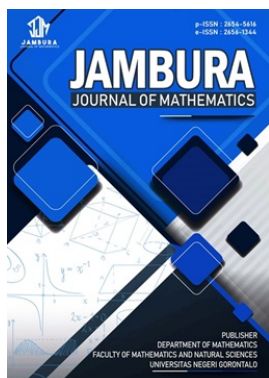


	Homepage	:	<a href="http://ejournal.ung.ac.id/index.php/euler/index">http://ejournal.ung.ac.id/index.php/euler/index</a>
	Journal Abbreviation	:	Euler J. Ilm. Mat. Sains dan Teknol.
	Frequency	:	Three times a year
	Publication Language	:	English (preferable), Indonesia
	DOI	:	<a href="https://doi.org/10.37905/euler">https://doi.org/10.37905/euler</a>
	Online ISSN	:	2776-3706
	Editor-in-Chief	:	Resmawan
	Publisher	:	Department of Mathematics, Universitas Negeri Gorontalo
	Country	:	Indonesia
	OAI Address	:	<a href="http://ejournal.ung.ac.id/index.php/euler/oai">http://ejournal.ung.ac.id/index.php/euler/oai</a>
	Google Scholar ID	:	QF_r_gAAAAJ
	Email	:	<a href="mailto:euler@ung.ac.id">euler@ung.ac.id</a>

## JAMBURA JOURNAL • FIND OUR OTHER JOURNALS



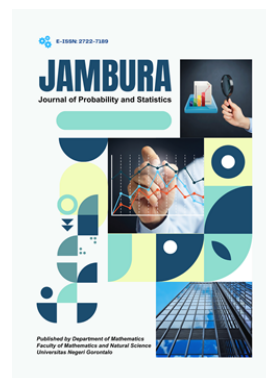
Jambura Journal of Biomathematics



Jambura Journal of Mathematics



Jambura Journal of Mathematics Education



Jambura Journal of Probability and Statistics

# Optimal Control for a COVID-19 and Tuberculosis Co-Infection Model with Asymptomatic COVID-19 Carriers

Sailah Ar Rizka<sup>1,\*</sup>, Regina Wahyudyah Sonata Ayu<sup>2</sup>, Dewi Ika Ainurrofiqoh<sup>1</sup>, Merysa Puspita Sari<sup>1</sup>, Nadia Kholifia<sup>1</sup>

<sup>1</sup>Department of Mathematics, Universitas Jember, Jember, Indonesia

<sup>2</sup>Department of Mathematics, Universitas Palangka Raya, Palangka Raya, Indonesia

## ARTICLE HISTORY

Received 28 February 2025

Revised 19 April 2025

Accepted 23 April 2025

Published 25 April 2025

## KEYWORDS

Co-infection  
COVID-19  
Nonlinear ODE Model  
Optimal Control  
Tuberculosis

**ABSTRACT.** This study applies optimal control theory to a deterministic co-infection model of COVID-19 and tuberculosis (TB) with asymptomatic COVID-19 carriers, who are assumed to be less infectious. The optimal control strategy aims to minimize intervention costs and reduce infections by implementing five control measures, including prevention and vaccination of COVID-19, treatment of both symptomatic and asymptomatic COVID-19-infected individuals, treatment of COVID-19 and active TB co-infected individuals, and prevention of treatment failure in active TB cases. Pontryagin's minimum principle is used to characterize the necessary conditions for optimal control in reducing infections. Numerical results demonstrate the effectiveness of the optimal control strategy in suppressing diseases. The incremental cost-effectiveness ratio (ICER) for different combinations of control measures is evaluated, showing that the intervention strategy performs best when all control measures are used.



This article is an open access article distributed under the terms and conditions of the Creative Commons Attribution-NonCommercial 4.0 International License. *Editorial of EULER:* Department of Mathematics, Universitas Negeri Gorontalo, Jln. Prof. Dr. Ing. B. J. Habibie, Bone Bolango 96554, Indonesia.

## 1. Introduction

COVID-19 and Tuberculosis (TB) are two leading infectious killers in the world requiring serious and urgent mitigation intervention. According to [1], there is an increase in TB cases in 2021 following COVID-19 pandemic, with an estimated 10.6 million new cases of TB and an estimated 1.6 million deaths from TB. There were approximately 771 million confirmed cases of COVID-19 worldwide by 12 October 2023, contributing to 6.9 million deaths [2]. Both COVID-19 and TB primarily affect the lungs and have similar symptoms, such as cough, fever, and difficulty in breathing. In addition, both diseases are spread through respiratory droplets, although TB exhibits a prolonged incubation period and a later disease progression [3].

Co-infection of COVID-19 and TB is described as a disease caused by both *M. tuberculosis* and SARS-CoV-2 infection. The current study shows that co-infection of COVID-19 and TB is common worldwide, with nineteen countries reporting co-infected patients, among them both high- and low-TB-prevalence countries [4]. There is evidence that TB is a risk factor for severe COVID-19, and patients with COVID-19 and TB co-infection are more likely to have severe disease and death than COVID-19 alone [5, 6]. Additionally, case studies have shown an increased risk of latent TB infections progressing to active TB following COVID-19 infection [7, 8]. The overlapping symptoms of COVID-19 and TB make diagnosis of co-infection difficult and may increase the severity of the disease. Early diagnosis of co-infection and proper medication may increase the patient's recovery rate and prevent further damage [9]. As COVID-19 and TB are becoming

public health issues, there is a need for serious attention to disease mitigation.

Mathematical modeling has been used to study the transmission dynamics of diseases [10–13], as well as co-infection of COVID-19 and TB, and to suggest appropriate control strategies to suppress the diseases. A compartmental co-infection model of COVID-19 and TB was developed in [14], suggesting that a decrease in contact rates with infectious individuals and an increase in treatments would reduce co-infection cases. [15] then proposed an optimal control problem by applying control measures, such as prevention and treatment for both COVID-19 and active TB, into [14] to minimize the number of infections. The co-infection model of COVID-19 and TB, which classifies infected individuals as reported and unreported cases, was developed in [16] and was extended to the optimal control problem by including awareness campaigns against TB in addition to other control measures. In [17], the co-infection model considered the order of co-infection of COVID-19 and TB and incorporated COVID-19 vaccination as a control measure in the optimal control problem. Unlike [17], COVID-19 vaccination in [18] was treated both as a compartment in the co-infection model and as a control measure, and it also took into account exogenous reinfection of TB.

As COVID-19 infection elevates the risk of progression of latent TB to active TB, it is important to properly mitigate both diseases and their co-infection. With this in mind, we propose an optimal control strategy to reduce the incidence of COVID-19, TB, and their co-infection. This strategy includes supervised treatment of active TB, implementation of preventive measures, vaccination, and medical treatment for COVID-19 and its co-infection

\*Corresponding Author.

with active TB. The control interventions are incorporated into a co-infection model of COVID-19 and TB in [19], which addresses imperfect vaccination for COVID-19 and asymptomatic COVID-19 individuals. Different from the model in [19], we consider the susceptibility of individuals vaccinated with COVID-19 to become infected with TB. This paper is structured as follows. In section 2, the method used in this study is explained. The findings of this study are then given in section 3, including model description in section 3.1, optimal control problem in section 3.2, and numerical results in section 3.3. In section 3.1, we present the co-infection model of COVID-19 and TB in [19] together with the parameter values, descriptions, and assumptions used. The existence and the invariant region of the solutions, demonstrating their biological relevance, are also analyzed. In section 3.2, the co-infection model with controls is formulated and the optimal control problem is proposed. The existence and characterization of the optimal control is then derived using Pontryagin's minimum principle. The numerical simulations of the different control strategies and the analysis of the cost-effectiveness are presented in section 3.3. Finally the conclusion is given in section 4.

## 2. Methods

This section discusses the method of optimal control used to mitigate the spread of co-infection of COVID-19 and TB. First, the co-infection model of COVID-19 and TB is presented in the form of a system of nonlinear differential equations. The assumptions and the parameter descriptions and values of the co-infection model are explained. The positivity and boundedness of the solution of the system are derived analytically to validate the biological relevance of the co-infection model. The disease-free equilibrium (DFE) point and the basic reproduction number describing epidemic transmissibility are determined. Then, the optimal control problem is posed. The time-dependent control functions, along with descriptions and constraints, are incorporated into the co-infection model. The resulting co-infection model with controls, also called state equation, can generally be written as

$$\dot{x}(t) = f(x(t), u(t)), \quad t \geq t_0,$$

where  $x \in \mathbb{R}^m$  represents the states (i.e., the population compartments) of the system and  $u \in \mathbb{R}^n$  represents the control functions. The objective function representing the quantity (i.e., number of infections, intervention cost) to be minimized is written in the form of a performance index

$$\mathcal{J} = \int_{t_0}^{t_f} g(x(t), y(t)) dt,$$

where  $t_f$  is the final time. The Hamiltonian is then defined by introducing a Lagrange multiplier  $\lambda \in \mathbb{R}^m$  as follows

$$\mathcal{H} = g(x(t), y(t)) + \lambda^T \cdot f(x(t), u(t)).$$

The next step is to define a costate equation as

$$\dot{\lambda} = -\frac{\partial \mathcal{H}}{\partial x}(x(t), u(t)),$$

which satisfies the transversality condition

$$\lambda(t_f) = 0.$$

The optimal control functions  $u^*$  are determined by using Pontryagin's minimum principle [20], that is, by solving the stationary condition

$$\frac{\partial \mathcal{H}}{\partial u} = 0.$$

Some intervention strategies are defined as combinations of the resulting optimal controls. The intervention strategies are then simulated using the Forward-Backward Sweep method [21] to see the effectiveness of the optimal controls in minimizing the objective function. The cost-effectiveness of each intervention strategy is then evaluated using the ICER [22].

## 3. Results and Discussion

### 3.1. Description of the Model

The co-infection model of COVID-19 and TB in [19] is being studied. The total population is grouped into ten compartments: susceptible individuals ( $S$ ), individuals vaccinated against COVID-19 ( $V$ ), exposed to COVID-19 individuals ( $E$ ), asymptomatic COVID-19 infected individuals ( $I_a$ ), symptomatic COVID-19 infected individuals ( $I_s$ ), latent TB infected individuals ( $L$ ), active TB infected individuals ( $A$ ), latent TB co-infected with COVID-19 individuals ( $I_{lc}$ ), active TB co-infected with COVID-19 individuals ( $I_{ac}$ ), and recovered individuals ( $R$ ). The total population  $N$  is given by

$$N = S + V + E + I_a + I_s + L + A + I_{lc} + I_{ac} + R. \quad (1)$$

The following system of nonlinear differential equations describes the co-infection dynamics of COVID-19 and TB.

$$\begin{aligned} \frac{dS}{dt} &= \Pi + \omega V + (\kappa_c + \kappa_t) R - (v + \mu + \alpha_c + \alpha_t) S, \\ \frac{dV}{dt} &= vS - [(1 - \varepsilon)\alpha_c + \alpha_t + \omega + \mu] V, \\ \frac{dE}{dt} &= \alpha_c S + (1 - \varepsilon)\alpha_c V - (\sigma_c + \mu) E, \\ \frac{dI_a}{dt} &= \sigma_c(1 - \psi) E - (\mu + \delta_c + \gamma_1 + \theta\alpha_t) I_a, \\ \frac{dI_s}{dt} &= \sigma_c\psi E + pI_{lc} + mI_{ac} - (\mu + \delta_c + \gamma_2 + \theta\alpha_t) I_s, \\ \frac{dL}{dt} &= \alpha_t S + \alpha_t V - (\sigma_t + \mu + \gamma_3 + \theta\alpha_c) L, \\ \frac{dA}{dt} &= \sigma_t L + qI_{lc} + nI_{ac} - (\mu + \delta_t + \gamma_4 + \theta\alpha_c) A, \\ \frac{dI_{lc}}{dt} &= \theta\alpha_t(I_a + I_s) + \theta\alpha_c L - (\mu + \delta_{ct} + \sigma_{ct} + p + q) I_{lc}, \\ \frac{dI_{ac}}{dt} &= \sigma_{ct} I_{lc} + \theta\alpha_c A - (\mu + \delta_{ct} + m + n) I_{ac}, \\ \frac{dR}{dt} &= \gamma_1 I_a + \gamma_2 I_s + \gamma_3 L + \gamma_4 A - (\mu + \kappa_c + \kappa_t) R, \end{aligned} \quad (2)$$

with the initial conditions

$$\{S(0) > 0, V(0) \geq 0, E(0) \geq 0, I_a(0) \geq 0, I_s(0) \geq 0, L(0) \geq 0, A(0) \geq 0, I_{lc}(0) \geq 0, I_{ac}(0) \geq 0, R(0) \geq 0\}. \quad (3)$$

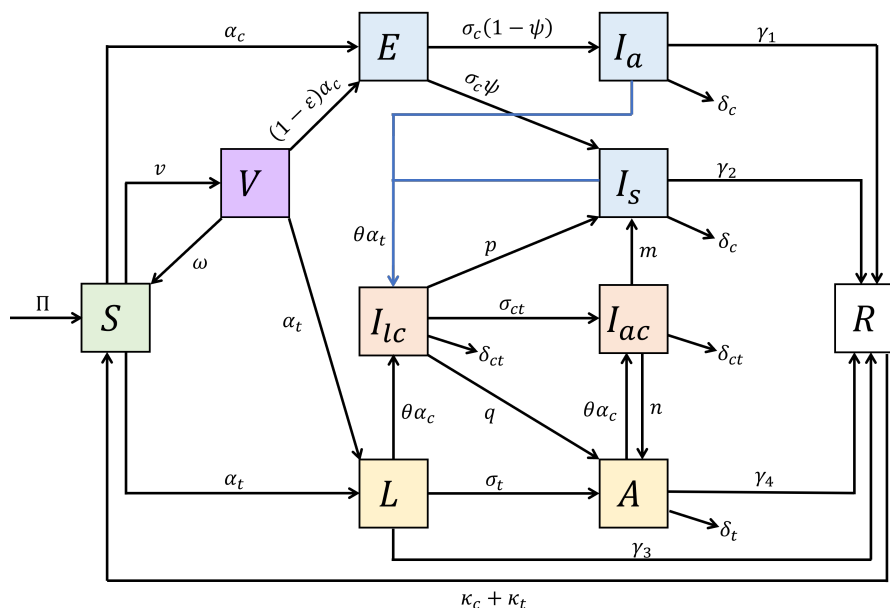


Figure 1. The co-infection diagram of COVID-19 and TB.

Figure 1 is a diagram depicting the co-infection dynamics of COVID-19 and TB. Table 1 describes the model parameters and their values.

In accordance with the model (2), the susceptible individuals are infected by COVID-19 and TB, respectively, at the rates  $\alpha_c$  and  $\alpha_t$  defined as follows.

$$\alpha_c = \frac{\beta_c(\eta I_a + I_s) + \beta_{ct}(I_{lc} + I_{ac})}{N},$$

$$\alpha_t = \frac{\beta_t A + \beta_{ct} I_{ac}}{N}.$$

That is, susceptible individuals can become infected with COVID-19 following exposure to either asymptomatic or symptomatic COVID-19 infected individuals and co-infected individuals ( $I_{lc}$  and  $I_{ac}$ ). The modification parameter  $\eta$  describes the lower infectiousness caused by asymptomatic individuals compared to symptomatic individuals. Additionally, susceptible individuals can become latent TB individuals after being exposed to active TB ( $A$ ) and active-TB co-infected with COVID-19 ( $I_{ac}$ ) individuals. The following are several assumptions used in the system (2).

1. Individuals with COVID-19 are susceptible to TB infection, likewise individuals with TB are susceptible to COVID-19 infection [5, 19, 23].
2. Exposed to COVID-19 individuals ( $E$ ) are not infectious.
3. Co-infection is more likely to occur after infection with either COVID-19 or TB. This is addressed by the enhancement factor of the co-infection rate  $\theta$ , where  $\theta \geq 1$  [19, 24, 25].
4. Co-infected individuals spread either COVID-19 or TB, but not both simultaneously [16, 19].
5. Co-infected individuals cannot recover from both COVID-19 and TB simultaneously, but recover from one disease at a time [14, 15]. That is, latent-TB co-infected with COVID-19 individuals recover from either TB at rate  $p$  or from COVID-19 at rate  $q$ . Meanwhile, active-TB co-infected with COVID-19 individuals recover from either TB at rate  $m$  or from COVID-19 at rate  $n$ .

6. There are disease-related deaths for asymptomatic and symptomatic COVID-19 infected individuals, active TB infected individuals, latent and active TB co-infected with COVID-19 individuals.
7. Individuals vaccinated against COVID-19 are susceptible to TB infection.

### 3.1.1. Positivity and Boundedness of Solutions

The following theorem analyzes the existence of solutions of the system (2) and the biological relevance of these solutions.

**Theorem 1.** *The dynamical system (2) has unique solutions that are positively invariant in the region*

$$\Gamma = \left\{ (S, V, E, I_a, I_s, L, A, I_{lc}, I_{ac}, R) \in \mathbb{R}_+^8 : 0 \leq N(t) \leq \frac{\Pi}{\mu} \right\}.$$

*Proof.* Let  $x = (S, V, E, I_a, I_s, L, A, I_{lc}, I_{ac}, R)$ . We write the system (2) as  $\dot{x} = f(x, t)$  where  $f(x, t)$  is the right hand side of the system (2). Note that  $f(x, t) \in C^1$  in  $\mathbb{R}_+^8$ . Hence by Picard-Lindöf theorem [26], the system (2) has unique solutions. To establish the positivity of the solutions of the system (2) with the given initial condition (3), note that

$$\frac{dS}{dt} > -(v + \mu + \alpha_c + \alpha_t) S.$$

Thus, we get

$$S(t) > S(0) \exp \left\{ - \int_0^t (v + \mu + \alpha_c + \alpha_t) \right\} > 0,$$

for all  $t \geq 0$ . In the same way, it can be proved that solutions for other states are positive for all  $t \geq 0$ . The rate of change of total

**Table 1.** The values and descriptions of the model parameters.

Parameter	Description	Value	Reference
$\Pi$	Recruitment rate of susceptible individuals ( $S$ )	$1.2 \times 10^4$	[19, 27]
$\eta$	Modification parameter of infection rate for the asymptomatic COVID-19 infected individuals ( $I_a$ )	0.45	[19, 28]
$v$	Vaccination rate against COVID-19	0.0203	[29]
$\beta_c$	Transmission coefficient of COVID-19	0.5249	[19, 27]
$\beta_t$	Transmission coefficient of TB	2.9598	[19, 30]
$\beta_{ct}$	Transmission coefficient of COVID-19 and TB co-infection	0.225	[19]
$p$	Recovery rate of $I_{lc}$ from TB	0.012	[18, 19]
$q$	Recovery rate of $I_{lc}$ from COVID-19	0.02095	[19, 30]
$m$	Recovery rate of $I_{ac}$ from TB	0.012	[18, 19]
$n$	Recovery rate of $I_{ac}$ from COVID-19	0.02095	[19, 30]
$\kappa_c$	Rate of immunity loss in individuals recovering from COVID-19	0.011	[19, 31]
$\kappa_t$	Rate of immunity loss in individuals recovering from TB	0.0027	[19, 32]
$\omega$	Waning rate of vaccine efficacy againts COVID-19	0.000297	[19, 27]
$\varepsilon$	Efficacy of the COVID-19 vaccine	0.7	[19, 27]
$\sigma_c$	Progression rate of COVID-19 from exposure ( $E$ ) to either $I_a$ or $I_s$	0.4	[19, 27]
$\sigma_t$	Progression rate from latent TB ( $L$ ) to active TB ( $A$ )	0.0039	[15, 19]
$\sigma_{ct}$	Progression rate of co-infection from $I_{lc}$ to $I_{ac}$	1.1148	[15, 19]
$\theta$	Modification parameter of co-infection rate	1.3	[18, 19]
$\psi$	Proportion of individuals $E$ that progress to $I_s$ .	0.6	[19, 33]
$\mu$	Rate of natural mortality	0.0003516	[19, 27]
$\delta_c$	Mortality rate due to COVID-19 infection	0.008	[19, 34]
$\delta_t$	Mortality rate due to TB infection	0.00032	[19, 30]
$\delta_{ct}$	Mortality rate due to co-infection	0.002	[15, 19]
$\gamma_1$	Recovery rate of individuals infected with asymptomatic COVID-19 ( $I_a$ )	0.13978	[19, 35]
$\gamma_2$	Recovery rate of individuals infected with symptomatic COVID-19 ( $I_s$ )	0.1	[19, 35]
$\gamma_3$	Recovery rate of individuals infected with latent TB ( $L$ )	0.09	[14, 19]
$\gamma_4$	Recovery rate of individuals infected with active TB ( $A$ )	0.35	[16, 19, 36]
$\phi_1$	Efficacy of control $u_1$ on $S$	0.5	Assumed
$\phi_2$	Efficacy of control $u_2$ on $I_s$	0.5	Assumed
$\phi_3$	Efficacy of control $u_3$ on $L$	0.5	Assumed
$\phi_4$	Efficacy of control $u_4$ on $A$	0.5	Assumed
$w_1$	Weighting cost on $u_1$	50	Assumed
$w_2$	Weighting cost on $u_2$	250	Assumed
$w_3$	Weighting cost on $u_3$	150	Assumed
$w_4$	Weighting cost on $u_4$	300	Assumed
$w_5$	Weighting cost on $u_5$	100	Assumed

population  $N(t)$  is given by

$$\frac{dN}{dt} = \Pi - \mu N - \delta_c (I_a + I_s) - \delta_t A - \delta_{ct} (I_{lc} + I_{ac}) < \Pi - \mu N.$$

This imply that

$$N(t) < N(0) e^{-\mu t} + \frac{\Pi}{\mu} (1 - e^{-\mu t}).$$

Thus, as  $t \rightarrow \infty$ , for  $N(0) > 0$ , we have  $N(t) < \frac{\Pi}{\mu}$ . It means that all solutions of the system (2) are positively invariant in  $\Gamma$ .  $\square$

As all solutions of the system (2) are positively invariant, this means that the COVID-19 and TB co-infection model is epidemiologically well-posed in mathematical perspective.

### 3.1.2. Basic Reproduction Number

The co-infection system of COVID-19 and TB (2) has a disease-free equilibrium (DFE) given by

$$E_0 = (S^*, V^*, E^*, I_a^*, I_s^*, L^*, A^*, I_{lc}^*, I_{ac}^*, R^*) = \left( \frac{\pi(\omega + \mu)}{\mu(v + \omega + \mu)}, \frac{\pi v}{\mu(v + \omega + \mu)}, 0, 0, 0, 0, 0, 0, 0, 0 \right).$$

By the use of the next generation matrix operator [37], the following basic reproduction number is obtained.

$$R_0 = \max\{R_0^C, R_0^T\}, \tag{4}$$

where

$$R_0^C = \beta_c \sigma_c \frac{(\omega + \mu + (1 - \varepsilon)v)}{(v + \omega + \mu)(\sigma_c + \mu)} \left( \frac{\eta(1 - \psi)}{\mu + \delta_c + \gamma_1} + \frac{\psi}{\mu + \delta_c + \gamma_2} \right),$$

$$R_0^T = \frac{\beta_t \sigma_t}{(\mu + \gamma_3 + \sigma_t)(\mu + \delta_t + \gamma_4)}.$$

This basic reproduction number tells the tendency of the diseases to be endemic or to vanish. That is, the diseases will be endemic if  $R_0 > 1$  and will vanish if  $R_0 < 0$ .

### 3.2. Optimal Control Problem

This section presents the optimal control problem along with its objective and constraints. We add five time-dependent control functions  $u_i$ , for  $i = 1, 2, 3, 4, 5$ , to the system (2) as follows.

1.  $u_1$  represents the preventive measures taken to reduce the contact between healthy individuals and those infected with COVID-19, including the frequent washing of hands, the use of antiseptics and masks, the avoidance of public gatherings, and the imposition of travel restrictions. Hence, we modify the COVID-19 infection rate as  $(1 - \phi_1 u_1) \alpha_c$ , where the effectiveness of the control  $u_1$  is  $\phi_1$ .
2.  $u_2$  represents the measures taken to optimize the treatment for patients with COVID-19, both asymptomatic ( $I_a$ ) and symptomatic ( $I_s$ ) individuals. This includes the provision of concentrated isolation facilities for COVID-19 patients who are either asymptomatic or exhibiting mild symptoms and the increase in bed capacities at hospitals for patients with severe COVID-19. The effectiveness of the control  $u_2$  is  $\phi_2$ .
3.  $u_3$  represents the treatment for individuals co-infected with COVID-19 and active TB ( $I_{ac}$ ), where the efficacy is  $\phi_3$ . The treatment combines the recommended TB regimen with the standard COVID-19 treatment [38]. This implies that co-infected individuals recover from either TB or COVID-19 at a rate of  $(1 + \phi_3 u_3) m$  and  $(1 + \phi_3 u_3) n$ , respectively.
4.  $u_4$  represents the efforts to prevent treatment failure in patients with active TB ( $A$ ), e.g., by supervising patients, helping them to take their TB medicines regularly, and completing TB treatment. The effectiveness of the control  $u_4$  is  $\phi_4$ .
5.  $u_5$  represents COVID-19 vaccination for susceptible individuals ( $S$ ).

The mathematical model representing the co-infection of COVID-19 and TB with controls, is given by the following system of nonlinear ordinary differential equations.

$$\begin{aligned} \frac{dS}{dt} &= \Pi + \omega V + (\kappa_c + \kappa_t) R \\ &\quad - (v + u_5 + \mu + (1 - \phi_1 u_1) \alpha_c + \alpha_t) S, \\ \frac{dV}{dt} &= (v + u_5) S - [(1 - \varepsilon) (1 - \phi_1 u_1) \alpha_c + \alpha_t + \omega + \mu] V, \\ \frac{dE}{dt} &= (1 - \phi_1 u_1) \alpha_c S + (1 - \varepsilon) (1 - \phi_1 u_1) \alpha_c V - (\sigma_c + \mu) E, \\ \frac{dI_a}{dt} &= \sigma_c (1 - \psi) E - (\mu + \delta_c + \gamma_1 + \phi_2 u_2 + \theta \alpha_t) I_a, \\ \frac{dI_s}{dt} &= \sigma_c \psi E + p I_{lc} + m (1 + \phi_3 u_3) I_{ac} \\ &\quad - (\mu + \delta_c + \gamma_2 + \phi_2 u_2 + \theta \alpha_t) I_s, \\ \frac{dL}{dt} &= \alpha_t S + \alpha_t V - (\sigma_t + \mu + \gamma_3 + \theta (1 - \phi_1 u_1) \alpha_c) L, \\ \frac{dA}{dt} &= \sigma_t L + q I_{lc} + n (1 + \phi_3 u_3) I_{ac} \\ &\quad - (\mu + \delta_t + \gamma_4 + \phi_4 u_4 + \theta (1 - \phi_1 u_1) \alpha_c) A, \\ \frac{dI_{lc}}{dt} &= \theta \alpha_t (I_a + I_s) + \theta (1 - \phi_1 u_1) \alpha_c L \\ &\quad - (\mu + \delta_{ct} + \sigma_{ct} + p + q) I_{lc}, \\ \frac{dI_{ac}}{dt} &= \sigma_{ct} I_{lc} + \theta (1 - \phi_1 u_1) \alpha_c A \end{aligned}$$

$$\begin{aligned} &\quad - (\mu + \delta_{ct} + (1 + \phi_3 u_3) (m + n)) I_{ac}, \\ \frac{dR}{dt} &= (\gamma_1 + \phi_2 u_2) I_a + (\gamma_2 + \phi_2 u_2) I_s + \gamma_3 L \\ &\quad + (\gamma_4 + \phi_4 u_4) A - (\mu + \kappa_c + \kappa_t) R. \end{aligned} \tag{5}$$

We consider the set of admissible control functions as follows.

$$\begin{aligned} \Omega &= \{u = (u_1(\cdot), u_2(\cdot), u_3(\cdot), u_4(\cdot), u_5(\cdot)) \\ &\quad \in (\mathbb{L}^\infty(0, T))^5 \mid 0 \leq u_i(t) \leq 1, \forall t \in [0, T], i = 1, \dots, 5\}. \end{aligned} \tag{6}$$

In this form, if the control  $u_i$  is zero, no effort is made to reduce infections. Conversely, if the control  $u_i$  is equal to one, the measure of effort made is equal to the effectiveness of the associated control  $\phi_i$ . As in the model (5), the rate of COVID 19 vaccination is influenced by both  $v$  and  $u_5$ . We assume that  $0 \leq u_5 \leq 1 - v$ , ensuring that the model (5) is more medically plausible. This implies that the vaccination rate against COVID-19 is at most 1.

The goal is to minimize the number of individuals suffering from the diseases in the compartments  $E, I_a, I_s, L, A, I_{lc}, I_{ac}$ , and the cost of implementing interventions associated with the controls  $u_i, i = 1, 2, 3, 4, 5$ . The objective function we consider here is given by

$$\begin{aligned} \mathcal{J}(u) &= \int_0^T E(t) + I_a(t) + I_s(t) + L(t) + A(t) \\ &\quad + I_{lc}(t) + I_{ac}(t) + \frac{1}{2} \sum_{i=1}^5 w_i u_i^2 dt, \end{aligned} \tag{7}$$

where the constants  $w_i$ , for  $i = 1, 2, 3, 4, 5$ , are the weighting costs associated with the controls  $u_i$ , for  $i = 1, 2, 3, 4, 5$ , respectively. Therefore, the aim is to find the optimal value of the control  $u^* \in \Omega$  such that the associated state trajectories  $S^*, V^*, E^*, I_a^*, I_s^*, L^*, A^*, I_{lc}^*, I_{ac}^*$ , and  $R^*$  with initial conditions (3) are solutions of the system (5) on the time interval  $[0, T]$  and the objective function (7) is minimized, i.e.,

$$\mathcal{J}(u^*) = \min_{\Omega} \mathcal{J}(u). \tag{8}$$

Using Pontryagin's minimum principle [20], the problem is solved by minimizing the following Hamiltonian  $\mathcal{H}$ .

$$\begin{aligned} \mathcal{H} &= E(t) + I_a(t) + I_s(t) + L(t) + A(t) + I_{lc}(t) + I_{ac}(t) \\ &\quad + \frac{1}{2} \sum_{i=1}^5 w_i u_i^2 + \lambda^T(t) \cdot g(S, V, E, I_a, I_s, L, A, I_{lc}, I_{ac}, R), \end{aligned} \tag{9}$$

where  $g$  is the right-hand side of the system (5) and  $\lambda$  is a continuous mapping  $[0, T] \rightarrow \mathbb{R}^{10}$  where  $\lambda = (\lambda_1(t), \lambda_2(t), \dots, \lambda_{10}(t))$  called *adjoint vector*. The existence of such optimal control  $u^*$  and its characterizations are given in the following theorems.

**Theorem 2.** Given the objective function (7) subjected to the model with controls (5) on the time interval  $[0, T]$ , there exists optimal control  $u^* = (u_1^*, u_2^*, u_3^*, u_4^*, u_5^*) \in \Omega$  and associated state trajectories  $(S^*, V^*, E^*, I_a^*, I_s^*, L^*, A^*, I_{lc}^*, I_{ac}^*, R^*)$

such that

$$\mathcal{J}(u^*) = \min_{\Omega} \mathcal{J}(u).$$

*Proof.* The states of the system (5) are continuously differentiable. When the controls are absent, based on the theorem 1, the system (5) has continuous and bounded solutions. As a consequence, together with the admissible controls (6), the partial derivatives with respect to the states are bounded. This leads to the system (5) satisfying the Lipschitz condition with respect to the states. Hence, based on the Picard-Lindelöf theorem [26], the solutions of the system (5) with the associated control functions exist.

Note that the system (5) is written in linear form in terms of the control functions, where the coefficients are time and state dependent. Besides, the integrand of the objective function (7) is quadratic in the control functions and therefore convex in  $u$ . Therefore, it follows from [39] that optimal control  $u^*$  minimizing the objective function (7) exists.  $\square$

The necessary condition for optimality is provided by Pontryagin's minimum principle [20] as stated in the theorem below.

**Theorem 3.** Let  $u^* = (u_1^*, u_2^*, u_3^*, u_4^*, u_5^*)$  be the optimal control to the problem (5), (6), (8), and  $(S^*, V^*, E^* I_a^*, I_s^*, L^*, A^*, I_{lc}^*, I_{ac}^*, R^*)$  be the associated optimal states on the time interval  $[0, T]$ . Then, there exist adjoint functions  $\lambda_1, \lambda_2, \dots, \lambda_{10}$  satisfying

$$\begin{aligned} \frac{d\lambda_1}{dt} &= \lambda_1 (v + u_5 + \mu + (1 - \phi_1 u_1) \alpha_c + \alpha_t) - \lambda_2 (v + u_5) \\ &\quad - \lambda_3 (1 - \phi_1 u_1) \alpha_c - \lambda_6 \alpha_t, \end{aligned}$$

$$\begin{aligned} \frac{d\lambda_2}{dt} &= -\lambda_1 \omega + \lambda_2 [(1 - \varepsilon) (1 - \phi_1 u_1) \alpha_c + \alpha_t + \omega + \mu] \\ &\quad - \lambda_3 (1 - \varepsilon) (1 - \phi_1 u_1) \alpha_c - \lambda_6 \alpha_t, \end{aligned}$$

$$\frac{d\lambda_3}{dt} = -1 + \lambda_3 (\sigma_c + \mu) - \lambda_4 \sigma_c (1 - \psi) - \lambda_5 \sigma_c \psi,$$

$$\begin{aligned} \frac{d\lambda_4}{dt} &= -1 + \lambda_4 (\mu + \delta_c + \gamma_1 + \phi_2 u_2 + \theta \alpha_t) - \lambda_8 \theta \alpha_t \\ &\quad - \lambda_{10} (\gamma_1 + \phi_2 u_2), \end{aligned}$$

$$\begin{aligned} \frac{d\lambda_5}{dt} &= -1 + \lambda_5 (\mu + \delta_c + \gamma_2 + \phi_2 u_2 + \theta \alpha_t) - \lambda_8 \theta \alpha_t \\ &\quad - \lambda_{10} (\gamma_2 + \phi_2 u_2), \end{aligned}$$

$$\begin{aligned} \frac{d\lambda_6}{dt} &= -1 + \lambda_6 (\sigma_t + \mu + \gamma_3 + \theta (1 - \phi_1 u_1) \alpha_c) - \lambda_7 \sigma_t \\ &\quad - \lambda_8 \theta (1 - \phi_1 u_1) \alpha_c - \lambda_{10} \gamma_3, \end{aligned}$$

$$\begin{aligned} \frac{d\lambda_7}{dt} &= -1 + \lambda_7 (\mu + \delta_t + \gamma_4 + \phi_4 u_4 + \theta (1 - \phi_1 u_1) \alpha_c) \\ &\quad - \lambda_9 \theta (1 - \phi_1 u_1) \alpha_c - \lambda_{10} (\gamma_4 + \phi_4 u_4), \end{aligned}$$

$$\begin{aligned} \frac{d\lambda_8}{dt} &= -1 - \lambda_5 p - \lambda_7 q + \lambda_8 (\mu + \delta_{ct} + \sigma_{ct} + p + q) \\ &\quad - \lambda_9 \sigma_{ct}, \end{aligned}$$

$$\frac{d\lambda_9}{dt} = -1 - \lambda_5 m (1 + \phi_3 u_3) - \lambda_7 n (1 + \phi_3 u_3)$$

$$+ \lambda_9 (\mu + \delta_{ct} + (m + n) (1 + \phi_3 u_3)),$$

$$\frac{d\lambda_{10}}{dt} = -\lambda_1 (\kappa_c + \kappa_t) + \lambda_{10} (\mu + \kappa_c + \kappa_t), \tag{10}$$

subjected to the transversality conditions

$$\lambda_i(T) = 0, i = 1, 2, 3, \dots, 10. \tag{11}$$

Furthermore,

$$\begin{aligned} u_1^*(t) &= \min \left\{ \max \left\{ 0, \frac{\phi_1 \alpha_c [U_1]}{w_1} \right\}, 1 \right\}, \\ u_2^*(t) &= \min \left\{ \max \left\{ 0, \frac{\phi_2 [(\lambda_4 - \lambda_{10}) I_a + (\lambda_5 - \lambda_{10}) I_s]}{w_2} \right\}, 1 \right\}, \\ u_3^*(t) &= \min \left\{ \max \left\{ 0, \frac{\phi_3 (-\lambda_5 m - \lambda_7 n + \lambda_9 (m + n)) I_{ac}}{w_3} \right\}, 1 \right\}, \\ u_4^*(t) &= \min \left\{ \max \left\{ 0, \frac{\phi_4 (\lambda_7 - \lambda_{10}) A}{w_4} \right\}, 1 \right\}, \\ u_5^*(t) &= \min \left\{ \max \left\{ 0, \frac{(\lambda_1 - \lambda_2) S}{w_5} \right\}, 1 - v \right\}. \end{aligned} \tag{12}$$

with

$$\begin{aligned} U_1 &= (-\lambda_1 + \lambda_3) S + (-\lambda_2 + \lambda_3) (1 - \varepsilon) V + \theta (-\lambda_6 + \lambda_8) L \\ &\quad + \theta (-\lambda_7 + \lambda_9) A. \end{aligned}$$

*Proof.* The results follow from Pontryagin's minimum principle [20] by utilizing the Hamiltonian function  $\mathcal{H}$  in (9). It asserts that the optimal solutions are achieved by fulfilling the adjoint equation requirements

$$\begin{aligned} \frac{d\lambda_1}{dt} &= -\frac{\partial \mathcal{H}}{\partial S}, \quad \frac{d\lambda_2}{dt} = -\frac{\partial \mathcal{H}}{\partial V}, \quad \frac{d\lambda_3}{dt} = -\frac{\partial \mathcal{H}}{\partial E}, \quad \frac{d\lambda_4}{dt} = -\frac{\partial \mathcal{H}}{\partial I_a}, \\ \frac{d\lambda_5}{dt} &= -\frac{\partial \mathcal{H}}{\partial I_s}, \quad \frac{d\lambda_6}{dt} = -\frac{\partial \mathcal{H}}{\partial L}, \quad \frac{d\lambda_7}{dt} = -\frac{\partial \mathcal{H}}{\partial A}, \quad \frac{d\lambda_8}{dt} = -\frac{\partial \mathcal{H}}{\partial I_{lc}}, \\ \frac{d\lambda_9}{dt} &= -\frac{\partial \mathcal{H}}{\partial I_{ac}}, \quad \frac{d\lambda_{10}}{dt} = -\frac{\partial \mathcal{H}}{\partial R}, \end{aligned}$$

which leads to system (10) and satisfies the transversality conditions in eq. (11). Furthermore, the optimal control  $u^*$  is derived by minimizing the Hamiltonian  $\mathcal{H}$  with respect to  $u$ , which comes from the optimality conditions

$$\frac{\partial \mathcal{H}}{\partial u_1} = 0, \quad \frac{\partial \mathcal{H}}{\partial u_2} = 0, \quad \frac{\partial \mathcal{H}}{\partial u_3} = 0, \quad \frac{\partial \mathcal{H}}{\partial u_4} = 0, \quad \frac{\partial \mathcal{H}}{\partial u_5} = 0. \tag{13}$$

Taking into account the constraints on the control  $u$  in eq. (6), the optimal control  $u^*$  is then derived as in eq. (12).  $\square$

### 3.3. Numerical Results

The numerical results of implementing optimal control strategies for the co-infection model of COVID-19 and TB (5) subjected to the objective function (7) are presented. The state system (5), the adjoint system (10) along with the transversality condition (11), and the optimal controls (12) are solved numerically employing the Forward-Backward Sweep method presented in [21]. The values of parameters in the model (5) and the weighting

**Table 2.** Cost-effectiveness of different intervention strategies.

Strategy	Population size at final time ( $T$ )							Averted $\times 10^7$	Cost $\times 10^7$	ICER no.
	$E$	$I_a$	$I_s$	$L$	$A$	$I_{lc}$	$I_{ac}$			
No control	1,199,700	1,059,900	2,630,100	4,759,200	439,330	293,740	7,286,700			
A	12,182	17,484	40,574	5,986	103	2	468	17,591,871	89,150,000	6
B	149,380	158,470	322,950	9,899	193	26	1,253	17,026,499	83,143,000	5
C	1,084,400	989,720	2,533,500	4,582,500	433,100	226,620	4,724,500	3,094,330	1,913,500,000	7
D	24	17	32	475	8	1	34	17,668,079	6,575,800	4
E	18	14	26	449	8	1	32	17,668,122	5,012,200	3
F	14	10	21	427	7	1	30	17,668,160	4,680,700	2
G	7	6	12	159	3	1	9	17,668,473	4,471,600	1

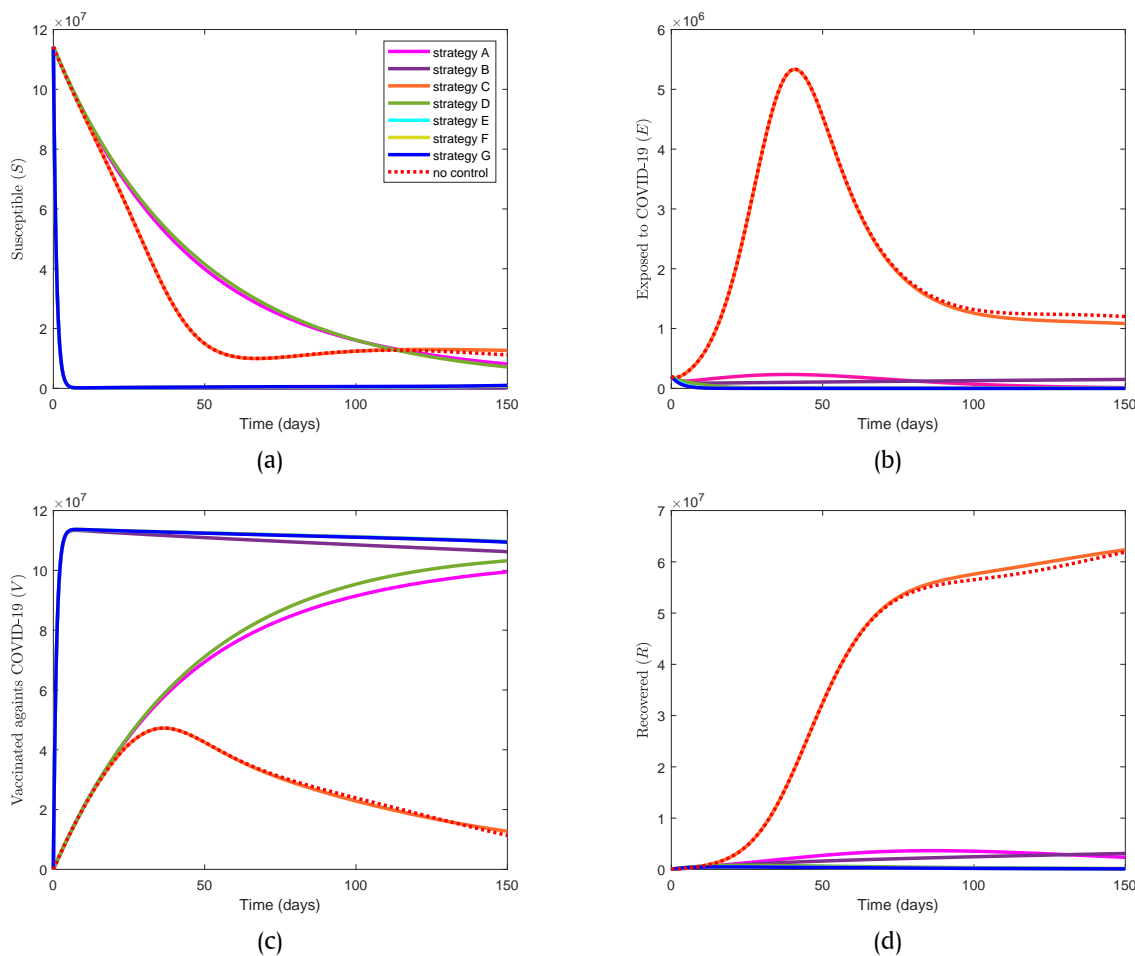


**Figure 2.** State solutions of the co-infected model: (a) susceptible ( $S$ ); (b) exposed ( $E$ ); (c) COVID-19 vaccinated ( $V$ ); and (d) recovered ( $R$ ) compartments when the seven strategies are implemented.

costs in the objective function (7) are given in the Table 1. The initial values of the states used in the simulation are assumed to be  $S(0) = 114227436$ ,  $V(0) = 0$ ,  $E(0) = 200000$ ,  $I_a(0) = 565$ ,  $I_s(0) = 80000$ ,  $L(0) = 100000$ ,  $A(0) = 30000$ ,  $I_{lc}(0) = 5000$ ,  $I_{ac}(0) = 500$ , and  $R(0) = 27058$ . There are seven different strategies that we consider here as we want to see how COVID-19 prevention ( $u_1$ ), COVID-19 and TB co-infection treatment ( $u_3$ ), and COVID-19 vaccination ( $u_5$ ) mitigate the spread of co-infection, in addition to the treatment of both asymptomatic and symptomatic COVID-19 individuals ( $u_2$ ) and active TB individuals ( $u_4$ ). The results of implementing the seven optimal control strategies are shown in Figure 2–Figure 4. Besides, the number of individuals in infected compartments at the end of simulation

is given in Table 2.

### 3.3.1. Strategy A ( $u_1 \neq 0$ )

In this strategy, COVID-19 prevention ( $u_1$ ) is implemented while other intervention controls are set to zero. Due to the control strategy, all COVID-19 infected compartments, including exposed ( $E$ ), COVID-19 infected ( $I_a$  and  $I_s$ ), and COVID-19 and TB co-infected ( $I_{lc}$  and  $I_{ac}$ ), are significantly reduced compared to no control, as shown in Figure 2 (b) and Figure 3. This strategy then results in far fewer individuals in the recovered compartment ( $R$ ) compared to no control, as the number of infected individuals to be treated decreases. Also, the number of susceptible individuals ( $S$ ) gradually decreases as many of them move to

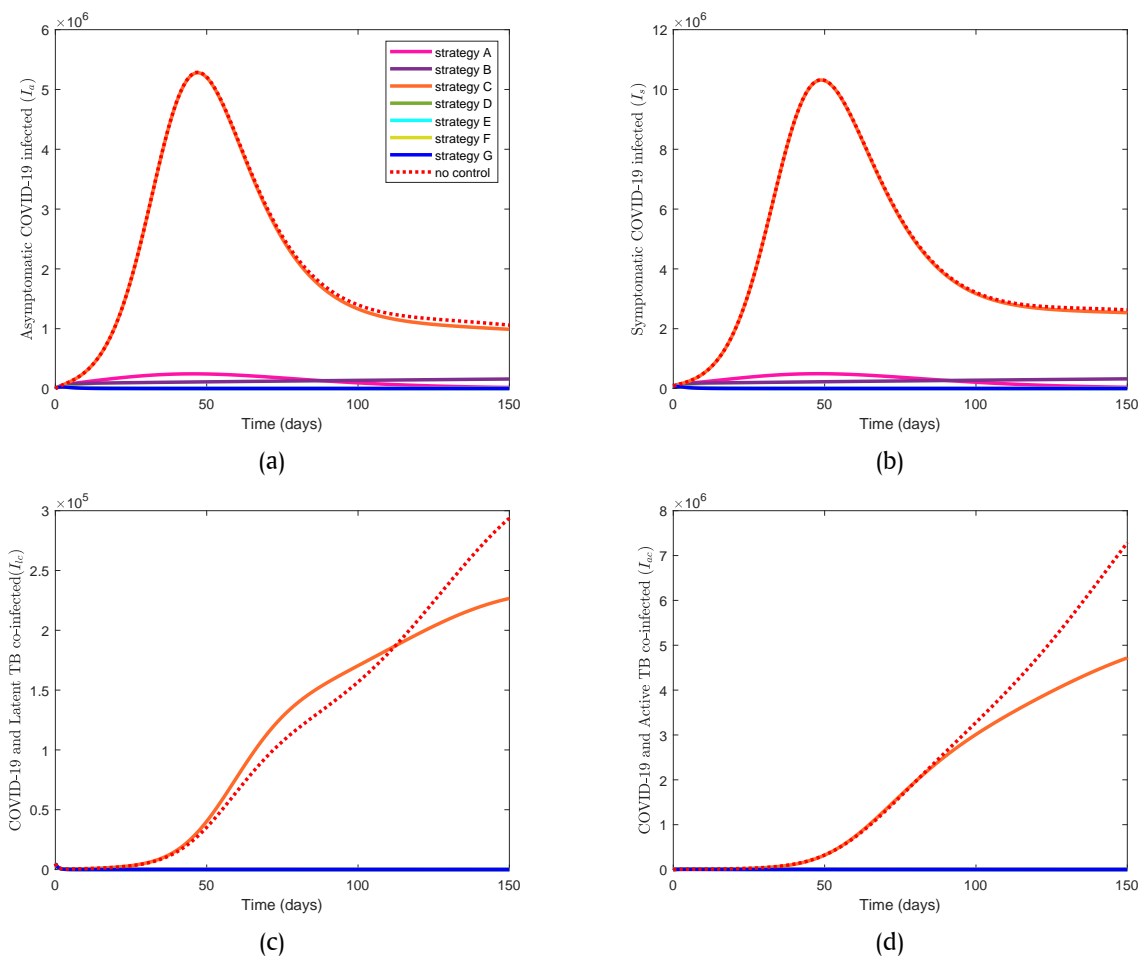


**Figure 3.** State solutions of the co-infected model: (a) asymptomatic COVID-19-infected ( $I_a$ ); (b) symptomatic COVID-19-infected ( $I_s$ ); (c) COVID-19 and latent TB co-infected ( $I_{ic}$ ); and (d) COVID-19 and active TB co-infected ( $I_{ac}$ ) compartments when the seven strategies are implemented.

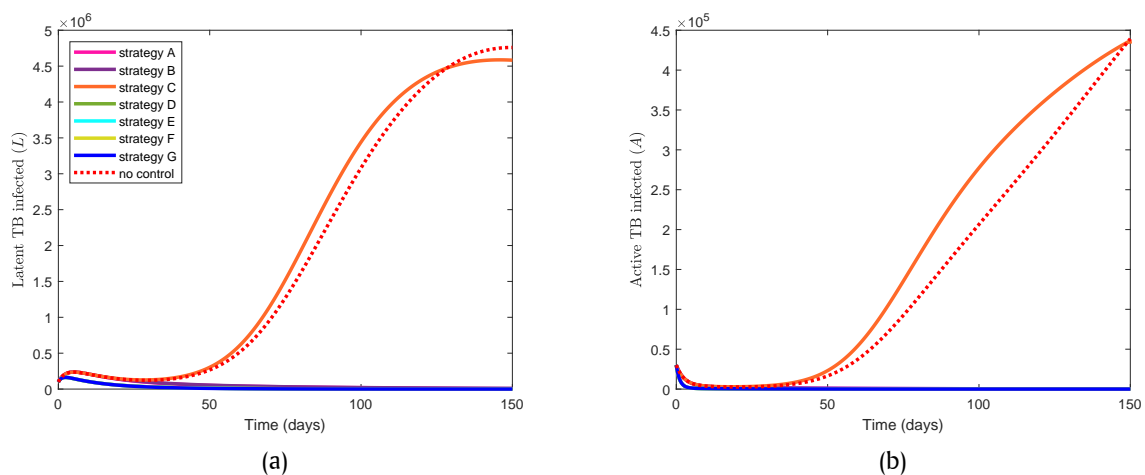


**Figure 4.** State solutions of the co-infected model: (a) latent TB ( $L$ ) and (b) active TB ( $A$ ) compartments when the seven strategies are implemented.

the COVID-19 vaccinated compartment ( $V$ ). As shown in Table 2, at the end of the simulation, the number of infected individuals is still in the thousands, especially the number of symptomatic COVID-19 infected individuals ( $I_s$ ) which is 40,574. The control profile for this strategy is shown in Figure 5 (a), which shows that

control  $u_1$  is at its maximum value 1 throughout the simulation.

### 3.3.2. Strategy B ( $u_5 \neq 0$ )

In this strategy, COVID-19 vaccinations ( $u_5$ ) are used to minimize the objective function (7), while the other controls are

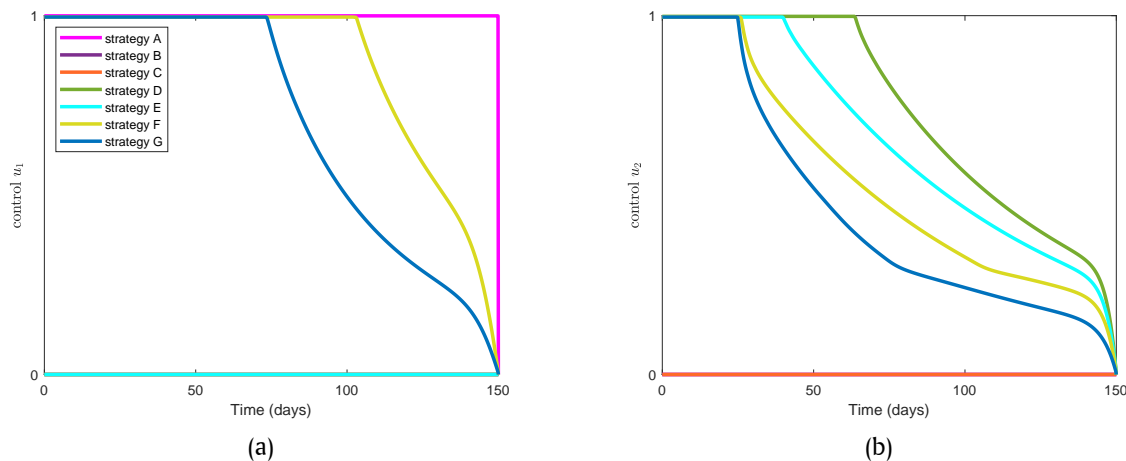


Figure 5. Control profiles: (a)  $u_1$  dan (b)  $u_2$  for all the seven strategies.

set to zero. The control profile  $u_5$  used in this strategy is shown in Figure 6 (c), which indicates that the control is at its maximum value  $1 - v$  throughout the simulation. This strategy results in an increase in the number of COVID-19 vaccinated individuals ( $V$ ) from the beginning of the simulation, as shown in Figure 2 (c). However, COVID-19 vaccination alone is not sufficient to contain the spread of the diseases. From Figure 2 (b) and Figure 3 (a)–(b), it can be seen that the number of exposed ( $E$ ), asymptomatic ( $I_a$ ), and symptomatic ( $I_s$ ) COVID-19 infections increases with the simulation time, although it is much lower compared to when no control is implemented.

### 3.3.3. Strategy C ( $u_3 \neq 0$ )

In this strategy, the spread of the diseases is controlled by providing treatment ( $u_3$ ) to individuals co-infected with both COVID-19 and active TB ( $I_{ac}$ ). As shown in Figure 3 (d), the number of  $I_{ac}$  individuals starts to differ significantly from those without control after 90 days, but with an increasing trend. The similar decrease can also be seen for individuals co-infected with both COVID-19 and latent TB ( $I_{lc}$ ), as shown in Figure 3 (c). On the other hand, Table 2 shows that control measures  $u_3$  alone are not sufficient to suppress COVID-19 and active TB co-infections, as the number of  $I_{ac}$  individuals when the simulation ends is higher compared to other strategies. This strategy also does not have much effect on mitigating other compartments, as their dynamics are not much different from those without control, as shown in Figure 2 – Figure 4. This indicates the need for additional interventions other than control effort  $u_3$ . The optimal treatment  $u_3$  for  $I_{ac}$  individuals is at its maximum value 1 throughout the simulation as shown in Figure 6 (a).

### 3.3.4. Strategy D ( $u_2, u_4 \neq 0$ )

In this strategy, the interventions used to control the diseases are treatments for both asymptomatic and symptomatic COVID-19-infected individuals ( $u_2$ ) and for active TB individuals ( $u_4$ ). As shown in Figure 2 (b) and Figure 3–Figure 4, all infected compartments, including exposed ( $E$ ), COVID-19 infected ( $I_a$  and  $I_s$ ), COVID-19 and TB co-infected ( $I_{lc}$  and  $I_{ac}$ ), and both latent and active TB ( $L$  and  $A$ ), are significantly reduced compared to those with no control. The decrease is also seen in the recov-

ered compartment ( $R$ ) as the number of infected individuals to be treated also decreases. The increase in the COVID-19 vaccinated compartment ( $V$ ) is due to the decreasing number of susceptible individuals ( $S$ ) being infected with the diseases. The implemented controls are shown in Figure 5 (b) and Figure 6 (b). The controls  $u_2$  and  $u_4$  are at the maximum value 1 for approximately 63 days and 14 days, respectively, and start to diminish gradually towards the end of the simulation.

### 3.3.5. Strategy E ( $u_2, u_4, u_5 \neq 0$ )

This strategy includes treatment of both asymptomatic and symptomatic COVID-19-infected individuals ( $u_2$ ), treatment of active TB individuals ( $u_4$ ), and COVID-19 vaccination ( $u_5$ ). The implementation of the  $u_5$  control gives rise to the number of susceptible individuals vaccinated against COVID-19 (progress to the  $V$  compartment) from the start of the simulation. This then has a significant decrease on the number of infected individuals, including exposed ( $E$ ), COVID-19 infected ( $I_a$  and  $I_s$ ), COVID-19 and TB co-infected ( $I_{lc}$  and  $I_{ac}$ ), and both latent and active TB ( $L$  and  $A$ ), as shown in Figure 2 (b) and Figure 3–Figure 4. The number of recovered individuals ( $R$ ) also decreases as the number of infected individuals to be treated decreases, as shown in Figure 2 (d). The control profiles of this strategy are shown in Figure 5 (b) and Figure 6 (c)–(d). It can be seen that the controls  $u_2$ ,  $u_4$  and  $u_5$  are at the maximum value for about 39 days, 13 days, and 6 days respectively and start to decrease gradually towards the end of the simulation as the number of infections decreases.

### 3.3.6. Strategy F ( $u_1, u_2, u_4, u_5 \neq 0$ )

This strategy implements all control measures except treatment for individuals co-infected with COVID-19 and TB, which is set to zero ( $u_3 = 0$ ). The profiles for each control measure are shown in Figure 5 and Figure 6 (b)–(c). It is observed that the maximum values of the control measures  $u_1$ ,  $u_2$ ,  $u_4$ , and  $u_5$  are at about 103 days, 26 days, 14 days, and 5 days, respectively. The dynamics of the compartments in this strategy do not differ much from those of strategy E. However, the additional COVID-19 prevention ( $u_1$ ) in this strategy results in the lower numbers of individuals in the infected compartments than that of strategy E in the end of simulation, as shown in Table 2. This can be seen

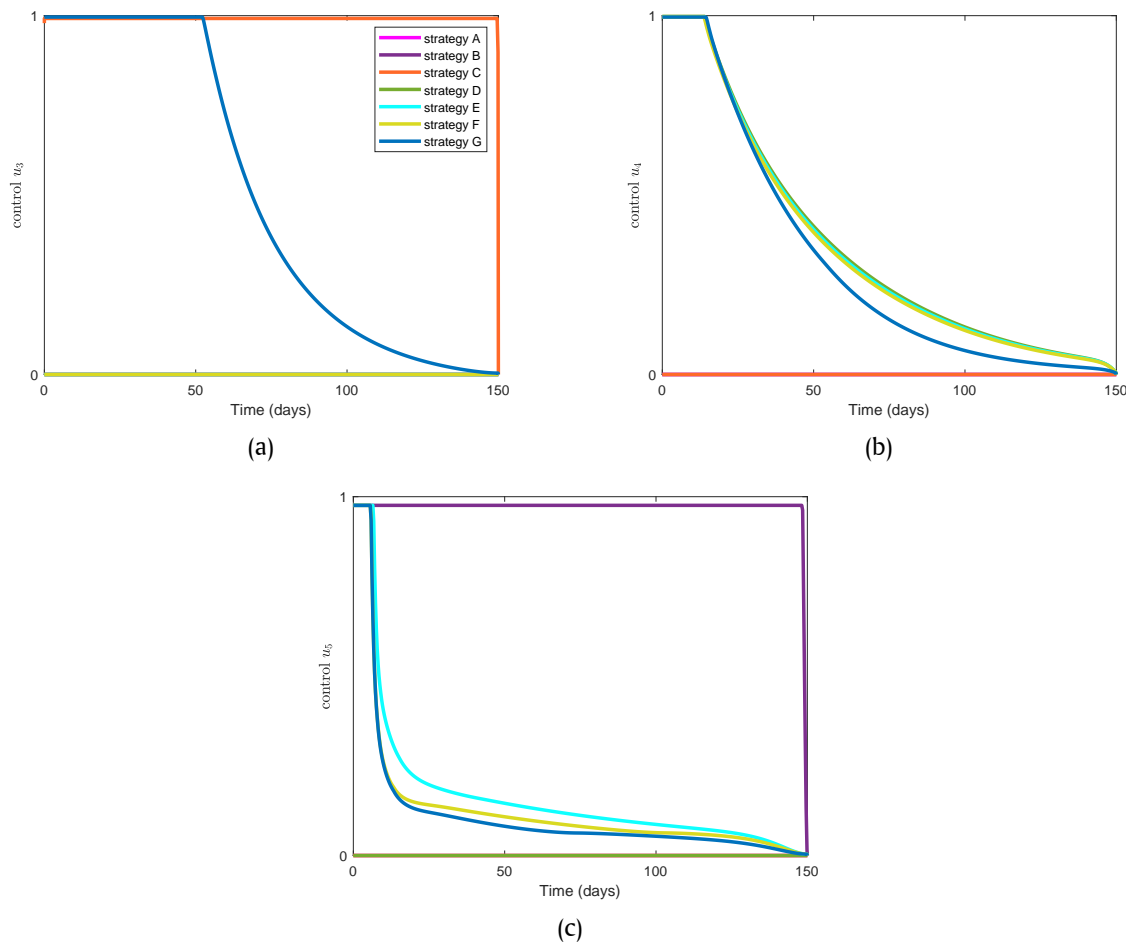


Figure 6. Control profiles: (a)  $u_3$ , (b)  $u_4$ , and (c)  $u_5$  for all the seven strategies.

from the number of infections averted by strategy F, 17,668,160, which is more than those averted by strategy E.

### 3.3.7. Strategy G ( $u_1, u_2, u_3, u_4, u_5 \neq 0$ )

In this strategy, all control measures  $u_1, u_2, u_3, u_4$ , and  $u_5$  are applied to the model. The number of exposed ( $E$ ), asymptomatic ( $I_a$ ), and symptomatic ( $I_s$ ) individuals infected with COVID-19 is significantly reduced compared to the case with no control, as shown in Figure 2 (b) and Figure 3 (a)–(b). A decrease is also observed in the number of individuals co-infected with COVID-19 and TB ( $I_{lc}, I_{ac}$ ), as shown in Figure 3 (c)–(d). In addition, Figure 4 shows that the number of latent and active TB individuals ( $L, A$ ) decreases in the short term without a peak compared to the one with no control. The control profiles in this strategy are shown in Figure 5 and Figure 6. We see that all the controls are at their maximum value from the beginning, with the COVID-19 prevention effort ( $u_1$ ) being the longest at about 73 days, while the other controls,  $u_2, u_3, u_4$ , are at about 24 days, 52 days, 14 days, and 6 days, respectively. All controls start to decrease gradually as the number of individuals in infected compartments decreases.

### 3.3.8. Comparison of Different Intervention Strategies

The seven intervention strategies have already been described. To compare the efficiency of the interventions in control-

ling the epidemic, the incremental cost-effectiveness ratio (ICER) [22] is used. The ICER allows the incremental cost-effectiveness of an intervention to be compared with that of a less effective alternative. The ICER [22] formula is as follows.

$$ICER = \frac{\text{difference in intervention costs}}{\text{difference in the total number of infection averted}}$$

The total number of averted infections is defined as the difference between the number of new infections with control and without control at the end of the simulation. Table 2 shows the ICER ranking. Table 2 shows that single control strategies A, B, and C are the three lowest cost interventions among the others, with strategy C being the least effective. It is seen from these three strategies that there are still significant numbers of individuals infected with either COVID-19 or TB in the final period, especially in the least effective strategy, C, with hundreds of thousands of individuals infected with the diseases. This indicates the need for combined interventions to mitigate the diseases. Meanwhile, strategy D performs quite well, as the number of infections averted does not differ much from the top three strategies, E, F, and G, although it is more costly than the other top three strategies. In addition, strategy G emerges as the most cost-effective intervention, with the highest number of infections averted at the lowest cost. Table 2 shows that the more control combinations there are, the more effective the strategies become, both in terms of disease aversion and cost spend. This shows that each

control measure has its own role in mitigating the co-infection epidemic of COVID-19 and TB.

#### 4. Conclusion

In this paper, we study and make some adjustments to the co-infection model of COVID-19 and TB in [19]. The properties of the model are investigated, including its existence, positivity, boundedness of solutions, and basic reproduction number. The co-infection model was extended to an optimal control problem by adding five control measures with the aim of mitigating the co-infection of COVID-19 and TB. The existence and characterization of optimal controls are presented analytically. The optimal characterizations are derived using Pontryagin's minimum principle. Numerical simulations of seven different intervention strategies are then performed to demonstrate the impact of optimal control in suppressing the diseases. The results of the intervention strategies are compared with the dynamics without control, which shows a significant reduction in the number of infection cases. The control profiles of each strategy show that interventions are applied at their maximum values from the beginning and gradually decrease as the diseases vanish. This suggests that maximum interventions should be applied from the beginning of the outbreak to effectively mitigate the diseases. In addition, the ICER evaluation shows that the intervention strategy with more control combinations leads to more cost-effective disease control strategies. It is shown that the strategy using all control measures performs best among the others in effectively and successfully reducing new infections. We note that the optimal control designed here is implemented in a deterministic model that doesn't take into account the uncertainties in the co-infection epidemic of COVID-19 and TB. Therefore, it is considered that a robust control should be developed in future work to address the uncertainties in the mitigation of the diseases.

**Author Contributions.** Sailah Ar Rizka: Conceptualization, Methodology, Software, Validation, Formal analysis, Investigation, Resources, Writing—original draft preparation, Visualization, Project administration. Regina Wahyudyah Sonata Ayu: Supervision, Methodology, Validation, Formal analysis, Investigation, Resources, Writing—original draft preparation. Dewi Ika Ainurofiqoh: Supervision, Validation, Resources, Investigation, Writing—review and editing. Merysa Puspita Sari: Software, Validation, Investigation, Writing—review and editing, Visualization. Nadia Kholifia: Software, Validation, Resources, Writing—review and editing, Visualization. All authors have read and approved the published version of the manuscript.

**Acknowledgement.** The authors are grateful to the editor and reviewers for their valuable critiques and recommendations, which significantly enhanced the quality of this work.

**Funding.** This research received no external funding.

**Conflict of interest.** The authors declare that there are no conflicts of interest related to this article.

**Data availability.** All data and materials supporting the findings of this study are publicly available and have been cited appropriately within the manuscript.

#### References

- [1] WHO, "Global tuberculosis report," 2022.
- [2] WHO, "WHO Coronavirus (COVID-19) dashboard," 2023. [Online]. Available: <https://covid19.who.int/>
- [3] WHO, "Global tuberculosis programme: Tuberculosis and COVID-19," 2020. [Online]. Available: <https://www.who.int/teams/global-tuberculosis-programme/covid-19>
- [4] Q. Wang, S. Guo, X. Wei, Q. Dong, N. Xu, H. Li, J. Zhao, and Q. Sun, "Global prevalence, treatment and outcome of tuberculosis and COVID-19 coinfection: a systematic review and meta-analysis," *BMJ Open*, vol. 12, no. 6, 2017, doi: 10.1136/bmjopen-2021-059396.
- [5] TB/COVID-19 Global Study Group, "Tuberculosis and COVID-19 co-infection: description of the global cohort," *The European respiratory journal*, vol. 59, no. 3, 2022, doi: 10.1183/13993003.02538-2021.
- [6] W. M. Song, J. Y. Zhao, Q. Y. Zhang, S. Q. Liu, X. H. Zhu, Q. Q. An, T. T. Xu, S. J. Li, J. Y. Liu, N. N. Tao, Y. Liu, Y. F. Li, and H. C. Li, "COVID-19 and Tuberculosis Coinfection: An Overview of Case Reports/Case Series and Meta-Analysis," *Frontiers in Medicine*, vol. 8, 2021, doi: 10.3389/fmed.2021.657006.
- [7] S. Colby and R. Shah, "TB reactivation following COVID-19 infection," *Chest*, vol. 162, no. 4, 2022, doi: 10.1016/j.chest.2022.08.255.
- [8] M. Khayat, H. Fan, and Y. Vali, "COVID-19 promoting the development of active tuberculosis in a patient with latent tuberculosis infection: A case report," *Respiratory Medicine Case Reports*, vol. 32, 2021, doi: 10.1016/j.rmcr.2021.101344.
- [9] P. Daneshvar, B. Hajikhani, F. Sameni, N. Noorisepehr, F. Zare, N. Bostan-shirin, S. Yazdani, M. Goudarzi, S. Sayyari, and M. Dadashi, "COVID-19 and tuberculosis coinfection: An overview of case reports/case series and meta-analysis of prevalence studies," *Heliyon*, vol. 9, no. 2, 2023, doi: 10.1016/j.heliyon.2023.e13637.
- [10] A. Ahmad, U. Atta, M. Farman, K. S. Nisar, H. Ahmad, and E. Hincal, "Investigation of lassa fever with relapse and saturated incidence rate: mathematical modeling and control," *Modelling Earth Systems and Environment*, vol. 11, no. 202, 2025, doi: 10.1007/s40808-025-02370-7.
- [11] M. Meena, M. Purohit, Shyamsunder, S. Purohit, D. Baleanu, and D. Suthar, "A novel fractionalized investigation of tuberculosis disease," *Applied Mathematics in Science and Engineering*, vol. 32, no. 1, 2024, doi: 10.1080/27690911.2024.2351229.
- [12] Shyamsunder, S. Bhattar, K. Jangid, A. Abidemi, K. Owolabi, and S. Purohit, "A new fractional mathematical model to study the impact of vaccination on COVID-19 outbreaks," *Decision Analytics Journal*, vol. 6, 2023, doi: 10.1016/j.dajour.2022.100156.
- [13] F. K. Alalhareth, U. Atta, A. H. Ali, A. Ahmad, and M. H. Alharbi, "Analysis of leptospirosis transmission dynamics with environmental effects and bifurcation using fractional-order derivative," *Alexandria Engineering Journal*, vol. 80, pp. 372–382, 2023, doi: <http://dx.doi.org/10.1016/j.aej.2023.08.063>.
- [14] K. G. Mekonen, S. F. Balcha, L. L. Obsu, and A. Hassen, "Mathematical modeling and analysis of TB and COVID-19 coinfection," *Journal of Applied Mathematics*, pp. 1–20, 2022, doi: 10.1155/2022/2449710.
- [15] K. G. Mekonen, L. L. Obsu, and T. G. Habtemichael, "Optimal control analysis for the coinfection of COVID-19 and TB," *Arab Journal of Basic and Applied Sciences*, vol. 29, no. 1, pp. 175–192, 2022, doi: 10.1080/25765299.2022.2085445.
- [16] M. S. Goudiaby, L. D. Gning, M. L. Diagne, B. M. Dia, H. Rwezaura, and J. M. Tchuente, "Optimal control analysis of a COVID-19 and tuberculosis co-dynamics model," *Informatics in Medicine Unlocked*, vol. 28, 2022, doi: 10.1016/j.imu.2022.100849.
- [17] A. B. Diabaté, B. Sangaré, and O. Koutou, "Optimal control analysis of a COVID-19 and Tuberculosis (TB) co-infection model with an imperfect vaccine for COVID-19," *SeMA Journal*, 2023, doi: 10.1007/s40324-023-00330-8.
- [18] Z. S. Kifle and L. L. Obsu, "Co-dynamics of COVID-19 and TB with COVID-19 vaccination and exogenous reinfection for TB: An optimal control application," *Infectious Disease Modelling*, vol. 8, no. 2, 2023, doi: 10.1016/j.idm.2023.05.005.
- [19] M. M. Ojo, O. J. Peter, E. F. D. Goufo, and K. S. Nisar, "A mathematical model for the co-dynamics of COVID-19 and tuberculosis," *Mathematics and Computers in Simulation*, vol. 207, pp. 499–520, 2023, doi: 10.1016/j.matcom.2023.01.014.
- [20] L. Pontryagin, V. Boltyanskii, R. Gramkrelidze, and E. Mischenko, *The mathematical theory of optimal processes*. New York – London: John Wiley & Sons, 1962, doi: 10.1002/zamm.19630431023.
- [21] S. Lenhart and J. T. Workman, *Optimal control applied to biological models*. New York: Chapman and Hall/CRC, 2007, doi: 10.1201/9781420011418.
- [22] G. G. Mwanga, H. Haario, and V. Capasso, "Optimal control problems of epi-

- demographic systems with parameter uncertainties: Application to a malaria two-age-classes transmission model with asymptomatic carriers," *Mathematical Biosciences*, vol. 261, pp. 1–12, 2015, doi: [10.1016/j.mbs.2014.11.005](https://doi.org/10.1016/j.mbs.2014.11.005).
- [23] M. S. Kumar, D. Surendran, M. S. Manu, P. S. Rakesh, and S. Balakrishnan, "Mortality due to TB-COVID-19 coinfection in India," *International Journal of Tuberculosis and Lung Disease*, vol. 25, no. 3, pp. 250–251, 2021, doi: [10.5588/ijtld.20.0947](https://doi.org/10.5588/ijtld.20.0947).
- [24] K. A. Alene, K. Wangdi, and A. C. A. Clements, "Impact of the COVID-19 pandemic on tuberculosis control: an overview," *Tropical Medicine and Infectious Disease*, vol. 5, no. 3, 2020, doi: [10.3390/tropicalmed5030123](https://doi.org/10.3390/tropicalmed5030123).
- [25] Y. Chen, Y. Wang, J. Fleming, Y. Yu, Y. Gu, C. Liu, L. Fan, X. Wang, M. Cheng, L. Bi, and Y. Liu, "Active or latent tuberculosis increases susceptibility to COVID-19 and disease severity," *MedRxiv*, 2020, doi: [10.1101/2020.03.10.20033795](https://doi.org/10.1101/2020.03.10.20033795).
- [26] B. J. Schroers, *Ordinary differential equations: a practical guide*. New York: Cambridge University Press, 2011, doi: [10.1017/CBO9781139057707](https://doi.org/10.1017/CBO9781139057707).
- [27] A. B. Gumel, E. A. Iboi, C. N. Ngonghala, and G. A. Ngwa, "Mathematical assessment of the roles of vaccination and non-pharmaceutical interventions on COVID-19 dynamics: a multigroup modeling approach," *MedRxiv*, pp. 1–24, 2021, doi: [10.1101/2020.12.11.20247916](https://doi.org/10.1101/2020.12.11.20247916).
- [28] F. B. Agosto, I. V. Erovenko, A. Fulk, Q. Abu-Saymeh, D. Romero-Alvarez, J. Ponce, S. Sindi, O. Ortega, J. M. S. Onge, and A. T. Peterson, "To isolate or not to isolate: The impact of changing behavior on COVID-19 transmission," *BMC Public Health*, vol. 22, no. 138, 2022, doi: [10.1186/s12889-021-12275-6](https://doi.org/10.1186/s12889-021-12275-6).
- [29] E. A. Iboi, C. N. Ngonghala, and A. B. Gumel, "Will an imperfect vaccine curtail the COVID-19 pandemic in the U.S.?" *Infectious Disease Modelling*, vol. 5, pp. 510–524, 2020, doi: [10.1016/j.idm.2020.07.006](https://doi.org/10.1016/j.idm.2020.07.006).
- [30] A. Omame, M. Abbas, and C. P. Onyenegecha, "A fractional-order model for COVID-19 and tuberculosis co-infection using Atangana-Baleanu derivative," *Chaos, Solitons, & Fractals*, vol. 153, 2021, doi: [10.1016/j.chaos.2021.111486](https://doi.org/10.1016/j.chaos.2021.111486).
- [31] M. L. Diagne, H. Rwezaura, S. Y. Tchoumi, and J. M. Tchuente, "A mathematical model of COVID-19 with vaccination and treatment," *Computational and Mathematical Methods in Medicine*, 2021, doi: [10.1155/2021/1250129](https://doi.org/10.1155/2021/1250129).
- [32] D. Okuonghae and S. E. Omosigho, "Analysis of a mathematical model for tuberculosis: What could be done to increase case detection," *Journal of Theoretical Biology*, vol. 269, no. 1, pp. 31–45, 2011, doi: [10.1016/j.jtbi.2010.09.044](https://doi.org/10.1016/j.jtbi.2010.09.044).
- [33] S. J. Brozak, B. Pant, S. Safdar, and A. B. Gumel, "Dynamics of COVID-19 pandemic in India and Pakistan: A metapopulation modelling approach," *Infectious Disease Modelling*, vol. 6, pp. 1173–1201, 2021, doi: [10.1016/j.idm.2021.10.001](https://doi.org/10.1016/j.idm.2021.10.001).
- [34] J. David, S. A. Iyanwura, P. Yuan, Tan, J. Kong, and H. Zhu, "Modeling the potential impact of indirect transmission on COVID-19 epidemic," *MedRxiv*, 2021, doi: [10.1101/2021.01.28.20181040](https://doi.org/10.1101/2021.01.28.20181040).
- [35] F. B. Agosto, E. Numfor, K. Srinivasan, E. A. Iboi, A. Fulk, J. M. S. Onge, and A. T. Peterson, "Impact of public sentiments on the transmission of COVID-19 across a geographical gradient," *PeerJ*, 2023, doi: [10.7717/peerj.14736](https://doi.org/10.7717/peerj.14736).
- [36] WHO, "Guidelines for the management of sexually transmitted infections," 2003.
- [37] P. Driessche and J. Watmough, "Reproduction numbers and sub-threshold endemic equilibria for compartmental models of disease transmission," *Mathematical biosciences*, vol. 180, no. 1–2, pp. 29–48, 2002, doi: [10.1016/S0025-5564\(02\)00108-6](https://doi.org/10.1016/S0025-5564(02)00108-6).
- [38] Q. Wang, Y. Cao, X. Liu, Y. Fu, J. Zhang, Y. Zhang, L. Zhang, X. Wei, and L. Yang, "Systematic review and meta-analysis of tuberculosis and COVID-19 co-infection: Prevalence, fatality, and treatment considerations," *PLoS Neglected Tropical Diseases*, vol. 18, no. 5, pp. 1–19, 2024, doi: [10.1371/journal.pntd.0012136](https://doi.org/10.1371/journal.pntd.0012136).
- [39] W. H. Fleming and R. W. Rishel, *Deterministic and stochastic optimal control*. New York: Springer, 2012, doi: [10.1007/978-1-4612-6380-7](https://doi.org/10.1007/978-1-4612-6380-7).